# Changes in detrital sediment supply to the central Yellow Sea since the Last Glacial Maximum

Hyo Jin Koo, Hyen Goo Cho

Department of Geology and Research Institute of Natural Science, Gyeongsang National University, Jinju 52828, Republic of
5  Korea

*Correspondence to*: Hyen Goo Cho (hgcho@gnu.ac.kr)

**Abstract.** The sediment supply to the central Yellow Sea since the Last Glacial Maximum was uncovered through clay mineralogy and geochemical analysis of core 11YS-PCL14 in the Central Yellow Sea mud (CYSM). The core can be divided into four units: Unit 4 (700–520 cm; 15.5–14.8 ka), Unit 3 (520–280 cm; 14.8–12.1 ka), Unit 2 (280–130 cm; 12.1–8.8 ka),

10  and Unit 1 (130–0 cm; < 8.8 ka). Comparison of the clay mineral compositions, rare earth elements, and εNd values indicated distinct provenance shifts in core PCL14. Moreover, the integration of clay mineralogical and geochemical indices showed different origins according to particle size. The late last deglaciation (Units 3 and 4) sediments originated from all potential provenance rivers, while the source of coarse sediments changed to Huanghe in Unit 3. Early Holocene (Unit 2) sediments were characterized by oscillating grain size, clay minerals, and moderate εNd values. In this period, the dominant fine sediment

15  provenance changed from the Huanghe to the Changjiang, whereas coarse sediments most likely originated from western Korean rivers. The Unit 1 CYSM sediments were sourced primarily from the Changjiang, along with minor contributions from the western Korean rivers. Possible transport mechanisms in the riverine sediment sources change and contributions to this include position shifts of river mouths, tidal stress evolution, and the development of the Yellow Sea Warm Current and coastal circulation systems.

**Keywords:** Central Yellow Sea mud (CYSM), clay mineralogy, sediment provenance, Sr–Nd isotopes, Rare earth elements

## 1 Introduction

The Yellow Sea, located between the China continent and Korean Peninsula, is a semi-enclosed epicontinental shelf with a complex oceanic circulation system (Fig. 1). It is notable for its large amount of runoff and terrigenous sediment supplied from several adjacent rivers, including two of the world's largest rivers, the Changjiang and Huanghe, as well as from several smaller Korean rivers, including the Han, Keum, and Yeongsan River. Although most riverine sediments are trapped in estuaries and along coastal areas, some are deposited on adjacent shelves (Milliman *et al.*, 1985; Milliman *et al.*, 1987), forming several shelf mud patch depositions such as Central Yellow Sea Mud (CYSM), Southeastern Yellow Sea Mud and Southwestern Cheju Island Mud (Fig 1). These deposits provide abundant information on paleo-environmental changes as well as sediment supply, marine hydrodynamics, and climate variation (*e.g.* Wang *et al.*, 1999; Kim and Kucera, 2000; Li *et al.*, 2014a; Cho *et al.*, 2015; Kwak *et al.*, 2016; Hu *et al.*, 2018).

The provenance of CYSM sediments have attracted many researchers over the last three decades. Many studies have indicated that CYSM sediments originated mostly from the Huanghe considering the large amount of sediment load carried by that river (Milliman *et al.*, 1987; Lee and Chough, 1989; Liu *et al.*, 2002; Yang and Liu, 2007; Shinn *et al.*, 2007; Xiang *et al.*, 2008). On the other hand, other studies have used mineralogical, geochemical, and magnetic observations and determined that the CYSM was formed from a complex mixture of sediments from the Huanghe as well as the Changjiang and several Korean rivers (Zhao *et al.*, 1990; Wei *et al.*, 2003; Zhang *et al.*, 2008; Li *et al.*, 2014a; Wang *et al.*, 2014; Koo *et al.*, 2018). In addition, recent studies using core sediments suggested that the provenance of CYSM changed mainly from Huanghe to Changjiang with minor contribution from the Korean rivers during the Holocene (Lim *et al.*, 2015; Hu *et al.*, 2018). However, the timing of the CYSM formation and the deposition environment prior to the Holocene are remains unclear.

Discrimination of sediment source and reconstruction of paleo-environmental changes can be undertaken based on grain size, clay mineralogy, and elemental signals. In particular, clay mineralogy and geochemistry have been utilized as a powerful tool to trace provenance of the terrigenous fraction of marine sediments in the Yellow sea (Yang *et al.*, 2002; Yang and Youn, 2007; Liu *et al.*, 2007, 2010b; Dou *et al.*, 2010; Hu *et al.*, 2012; Wang and Yang, 2013; Li *et al.*, 2014a; Koo *et al.*, 2018). Several additional factors can also control sedimentary characteristics, including terrigenous inputs, sea level and climate conditions (Wang et al., 1999; Duck et al., 2001; Hwang et al., 2014; Li et al., 2014a; Lim et al., 2015; Badejo et al., 2016; Hu et al., 2018). Particularly, paleo-river pathway associated with sea-level change that was recently reconstructed using high-resolution seismic data in the Yellow Sea can be explained reasonable for understanding CYSM formation during low stand period (KIGAM, 1993; Xu *et al.*, 1997; Yoo *et al.*, 2015, 2016).

In this study, we aimed to determine the sediment provenance and transport mechanism of CYSM using clay mineralogy and geochemistry multi-proxy. The purposes are to provide a broad insight into the supply of CYSM sediments and to reconstruct the paleo-environment since the last glacial maximum.

## 2. Oceanography

The Yellow Sea is characterized by a complex hydrodynamic system (Fig. 1), with two major circulation patterns. One is a basin-scale counterclockwise (cyclonic) gyre consisting of northward inflow via the Yellow Sea Warm Current (YSWC) in the central Yellow Sea and southward inflow via the Yellow Sea Coastal Current (YSCC) along the east coast of China (Beardsley *et al.*, 1985; Yang *et al.*, 2003) (Fig. 1). The other is a clockwise gyre in the eastern part made up of the YSWC and southward inflow from the Korea Coastal Current (KCC) (Beardsley *et al.*, 1985; Yang *et al.*, 2003). The YSWC is one of the most important dynamic phenomena in the East China Sea and Yellow Sea. It is a branch of the Kuroshio Current that carries warm, salty water into the Yellow Sea roughly along the Yellow Sea Trough (Xu *et al.*, 2009; Liu *et al.*, 2010a; Wang *et al.*, 2011, 2012). The Transversal Current (TC), identified in recent studies, separates from the KCC southwest of the Korean Peninsula, and some of its water flows northward along the YSWC (Lie *et al.*, 2013, 2016; Hwang *et al.*, 2014) (Fig. 1). The

Changjiang Diluted Water (CDW) that provides the most freshwater discharge into the Yellow Sea from the Changjiang spreads eastward, reaching as far as Cheju Island and Tsushima Strait (Hwang *et al*., 2014; Li *et al*., 2014a). The oceanic fronts include the Shandong Front (SDF), Jiangsu Coastal Front (JSCF) and Western Korean Coastal Front (WKCF) located in the

70 western and eastern boundaries of the Yellow Sea. These fronts play an important role in shaping Yellow Sea currents, as they separate different water masses (Huang *et al*., 2010; Li *et al*., 2014a) (Fig. 1).

## 3. Materials and methods

Core PCL14 (35°785' N, 124°115' E), which was 702 cm in length, was collected from CYSM at a water depth of approximately 80 m for multi-proxy paleo-environmental reconstruction. The core was subsampled at 10 cm intervals for grain

75 size, clay mineralogy and geochemical analyses.

The grain size and AMS$^{14}$C data were reported in Badejo *et al*. (2016). Radiocarbon ages for five selected depths (99 cm, 300 cm, 540 cm, 580 cm, and 698 cm) and the age-depth model was constructed based on the linear interpolation between the calibrated calendar ages (Badejo *et al*., 2016) (Table 1). The bottom of the core PCL14 dated approximately 15.5 ka, that PCL14 provides a continuous record of the late last deglaciation to Holocene in the CYSM.

80 The clay mineral analysis for was conducted using X-ray diffraction (XRD) on preferred-orientation specimens of clay-sized particles (< 2 μm) following the method in Cho et al. (2015). Semi-quantitative estimation of clay mineral abundances was completed using the Eva 3.0 program with the empirical factors from Biscaye (1965).

The composition of major and trace elements in 13 bulk samples was determined by Actlabs, Ontario, Canada, following the '4 LithoRes' methodology. The samples were fused using a lithium metaborate-tetraborate mixture. The melt produced by this

85 process was completely dissolved with 5% HNO$_3$. Major elements were analysed in the resulting solution by inductively coupled plasma-optical emission spectrometry (ICP-OES), with an analytical accuracy of < 6%. Trace element analyses were done by inductively coupled plasma-mass spectrometry (ICP-MS). The analytical reproducibility ranged between 5 and 12%. A total 18 samples of core PCL14 and riverine (Huanghe, Changjiang and Keum River) were selected for Sr–Nd isotopic analysis (Table 3). Sr–Nd isotopic measurements were performed on a thermal ionization mass spectrometry (TIMS) at the

90 Korea Basic Science Institute. Sr and Nd isotope ratios were normalized to $^{86}Sr/^{88}Sr = 0.1194$ and $^{146}Nd/^{144}Nd = 0.7219$, respectively. Analysis of the Sr standard NBS 987 and the Nd standard JNdi-1 resulted in $^{87}Sr/^{86}Sr = 0.710246 \pm 3$ (2SD, n = 10) and $^{143}Nd/^{144}Nd = 0.512115 \pm 6$ (2SD, n = 10). For convenience, the εNd parameter was calculated using a $^{143}Nd/^{144}Nd$ value of 0.512638 for the Chondritic Uniform Reservoir (Hamilton *et al*., 1983).

95 ## 4. Results

Core PCL14 could be divided mainly into four units considering downcore patterns especially mean grain size and clay mineral compositions (Figs. 2 and 3): Unit 4 (700–520 cm; 15.5–14.8 ka), Unit 3 (520–310 cm; 14.8–12.8 ka), Unit 2 (310–130 cm; 12.8–8.8 ka), and Unit 1 (130–0 cm; < 8.8 ka). In addition, Unit 2 could be subdivided into Unit 2-2 (310–210 cm; 12.8–10.5 ka), Unit 2-1 (210–130 cm; 10.5–8.8 ka) based on the variation trends. Wang *et al*. (2014) reported that the CYSM mud blanket

100 becomes thicker going westward based on a seismic profile. The mud layers in core sediments are thinner than expected from the seismic profile, but the trend is consistent (Fig. 2). Core EZ06-2, located east of PCL14, contains a 100-cm-thick mud layer, while YSC-1, to the west, has a 300-cm-thick layer (Fig. 2). The lower part of the mud layer is known as the transgressive deposit and contains many sands (Fig. 2). This coarse layer appears in all cores in the CYSM, with a boundary of ~10 ka (Li *et al*., 2014a; Lim *et al*., 2015). However, core PCL14 has additional mud layers with a high proportion of silt underneath the

105 transgressive deposit and a coarse layer at the bottom. Therefore, core PCL14 provides more records of the CYSM since the LGM, which could not be reconstructed in previous cores.

The vertical granularity, clay mineralogical, and geochemical characteristics of core PCL14 are plotted against the calibrated age on the $y$-axis in Fig. 3. The four clay minerals were dominated by illite (60.1–74.7%), followed by chlorite (12.0–22.6%), kaolinite (9.6–14.8%), and smectite (1.2–6.8%). The $^{87}Sr/^{86}Sr$ ratios ranged from 0.719 to 0.724 (mean 0.721) and the εNd
110   values from −16.2 to −12.3 (mean −14.0).

Tables 2 and 3 list the detailed characteristics of the clay minerals and geochemistry in each unit and their main potential provenances (the Huanghe, Changjiang, and western Korean rivers). Each unit had distinct dissimilarities in clay mineral content and mean grain size, especially the sand content (Fig. 2). The Unit 2 sediments were 1.8–44.2% (mean 17.6%) sand with a mean grain size of 6.6 φ (10.3 μm) and Unit 4 sediments had a high sand content (8–58.7%, mean 26.3%) with a mean
115   grain size of 6.0 Φ (15.6 μm). In comparison, Unit 1 contained only fine sediment with a mean grain size of 8.8 Φ (2.2 μm) and Unit 3 sediments were clayey silt with a mean grain size of 7.3 Φ (6.3 μm). The downcore variation in the clay mineral composition showed that the illite content decreased gradually from Unit 2 to 3 and was constant in the other parts of the core. Overall, the variations in the smectite and kaolinite+chlorite contents were opposite that of illite (Fig. 3). Units 3 and 4 had relatively constant compositions in terms of clay minerals, although their granularity was heterogeneous. The $^{87}Sr/^{86}Sr$ ratio
120   was constant at the bottom and tended to increase in the upper part. The εNd value was low in Units 2 and 4. ΣLREE/ΣHREE was low only in Unit 3, and was mostly constant.

## 5. Discussion

### 5.1. Provenance discrimination based on clay mineralogy

125   Relative clay mineral contents and ratios can be used as powerful proxies for determining fine-grained marine sediment provenance, especially in terms of the rivers from China and Korea that may contribute to CYSM (Yang *et al*., 2003; Choi *et al*., 2010; Li *et al*., 2014a; Xu *et al*., 2014; Lim *et al*., 2015; Kwak *et al*., 2016). Generally, Huanghe sediments are characterized by high smectite, and Changjiang sediments contain a lot of illite contents. Western Korean rivers (e.g. the Han, Keum, and Yeongsan) contain more kaolinite and chlorite than do Chinese rivers (Table 2).

130   A ternary diagram of smectite–(kaolinite+chlorite)–illite was utilized to determine the provenance of fine sediments in core PCL14 (Fig. 4). Although Unit 4 and 3 sediments differed in granularity, they had similar clay mineral compositions and plotted near the center of the three possible provenance end-members, indicating that clay-sized sediments were supplied with constant amounts from all potential rivers to the study area during these periods (Fig. 4a). Unit 2 sediments overall were characterized by an increasing illite content (Figs. 3 and 4b). It means that the influence of Changjiang-derived materials began
135   to increase during this period. However, Unit 2-2 sediments displayed an increase in smectite content with illite, and then every clay mineral composition except illite decrease in Unit 2-1 (Fig. 4b). Variation of smectite content in Unit 2 appears to be closely related to the change in coarse sediments (Figs. 3 and 4b). The relationship between smectite and coarse grains was also observed in the early Holocene sedimentary unit of core YSC-1 (Li *et al*., 2014a) and nearby core EZ06-2 between ~14.1 and ~9.0 ka (Lim *et al*., 2015). Unit 1 sediments had clay mineral compositions quite similar to those of Changjiang sediments,
140   indicating that they might be originate mainly from the Changjiang (Fig. 4b).

Consequently, clay mineralogical results were suggested that the finer detrital sediments in Units 3 and 4 were affected by all potential provenances. During Unit 2, the influence of the Changjiang increased gradually with temporary influx containing coarse particles and high smectite, and the later Unit 1 sediments were derived primarily from Changjiang inputs.

145   ### 5.2. Geochemical approaches

Geochemical proxies for provenance discrimination in the Yellow Sea have been investigated actively and verified by several studies (*e.g.* Yang *et al*., 2002; Xu *et al*., 2009; Song and Choi, 2009; Jung *et al*., 2012; Ha *et al*., 2013; Lim *et al*., 2015; Hu

*et al.*, 2018; Koo *et al.*, 2018). The chemical compositions of Korean and Chinese rivers differ, especially in their rare earth elements (REE) and Sr–Nd contents (Xu *et al.*, 2009; Jung *et al.*, 2012; Lim *et al.*, 2014; Hu *et al.*, 2018). These are essentially

150   unaltered during weathering, transport, and sedimentation, and can be a powerful tool for tracing the provenance of the terrigenous fraction of marine sediments (McLennan, 1989; Blum and Erel, 2003; Xu *et al.*, 2009).

Recent studies have emphasized that in addition to the source rock, many other factors influence the geochemical composition of riverine and marine sediments, such as grain size, heavy mineral content, and biogenic component, especially in bulk sediment analysis (Yang *et al.*, 2002; Song and Choi, 2009; Lim *et al.*, 2015; Hu *et al.*, 2018). For example, the major elements

155   Fe and Mg were suggested to be useful proxies in the Yellow Sea (Lim *et al.*, 2007). However, they are closely correlated with particle size because they are abundant in clay minerals, making them unconformable for provenance tracing in bulk sediments (Fig. 5a). In addition, Ca has a problem based on biogenic carbonate despite the poor correlation with grain size (Fig. 5a). Trace elements also exhibit positive and negative correlations with grain size (Yang *et al.*, 2002; Lim *et al.*, 2014). To complement this, recent studies have suggested ratios of the binding of abundant elements at comparable grain sizes (*e.g.*, the

160   La/Sc and Zr/Th ratios) (Yang *et al.*, 2002; Lim *et al.*, 2014). However, we observed that these ratios and mean grain size were strongly negatively correlated in our dataset (Fig. 5b), implying that these ratios are also unsuitable for studying provenance.

Normalization of REE values to upper continental crust (UCC) is a widely accepted method for discriminating the sediment provenances of various geological materials (Song and Choi, 2009; Xu et al., 2009; Lim *et al.*, 2015). This method can better offset differences caused by grain size, and could be a useful geochemical proxy (Fig. 5c). In addition, the Nd isotope ratio of

165   silicate particles is essentially unaltered during weathering, transport, and sedimentation and can be a powerful tool for tracing the provenance of the terrigenous fraction of marine sediments (Blum and Erel, 2003; Hu *et al.*, 2018). However, recent studies indicated that the Sr isotope composition in both Chinese and Korean riverine sediments was a function of grain size, with a higher $^{87}Sr/^{86}Sr$ in clay-dominated fractions than in silt-dominated fractions (Fig. 5d) (Hu *et al.*, 2018). Therefore, we used only the UCC-normalized REE and εNd values for discriminating sediment provenance; these could be useful indicators for

170   distinguishing the contributions of Chinese and Korean rivers.

Korean rivers are characterized by a high LREE and low εNd, while Chinese rivers have abundant MREE (middle REE) and εNd (Table 3, Fig. 6). Figs. 6 are discrimination plots using the REE and εNd values that clearly separate the Chinese and Korean rivers. In these plots, the REE values represented the source of both coarse and fine sediments because the analysis was performed with coarse grains. Unit 1 is generally close to the Changjiang with slightly influence of the Korean rivers, as

175   well as the clay mineralogy (Figs. 4 and 6). Unit 4 sediments are plotted between China and Korean river end-members in all discrimination plots (Fig. 6), consistent with the results for clay minerals, which suggests that the coarse sediments included in Unit 4 were from contributions from all potential rivers.

Interestingly, the clay-sized particles of Unit 2 were a composite of the Huanghe and Changjiang in Fig. 4, but the geochemical data were similar to Unit 4 (Fig. 6). This probably means that a significant amount of coarse sediments in Unit 2 was supplied

180   from Korean rivers with a high LREE (Fig. 6a). The association between an increased impact of Korean rivers and coarse sediments was identified in an isotope analysis before ~8 ka in core YSC-1 (Hu *et al.*, 2018). Thus, the supply of smectite in clay-sized particles and sand grains is synchronic, but possibly has different sources. In addition, Unit 3 sediments, identified as the homogenous origin as Unit 4 in clay mineralogy (Fig. 4), are biased towards Chinese rivers (Fig. 6), especially close to the Huanghe. A scatter plot of clay mineral ratio *vs.* εNd distinguished three possible provenances for particles smaller than

185   63 μm (Fig. 6c). Unit 3 sediments in this plot are certainly plotted close to the Huanghe. This is caused by the many silt fractions in Unit 3 and probably represents a relatively close supply from the Huanghe.

Consequently, the estimated sediment provenances in each unit based on the clay mineralogical and geochemical indices were as follows. During Unit 4, both coarse and fine sediments were influenced by all of these provenances. However, in Unit 3, silt-sized fractions were predominantly affected by the Huanghe. Unit 2 represented a period of great change in the sediment

190   sources. The fine grains in the Unit 2-2 sediments were derived primarily from Chinese rivers, especially the Huanghe, while

the Unit 2-1 samples were supplied mainly from the Changjiang, with minor contributions from the Huanghe and western Korean rivers. However, coarse sediments source in Unit 2 were identified as western Korean rivers based on geochemical indices. The source of CYSM sediments in Unit 1 was primarily the Changjiang.

### 5.3. Paleo-environmental implications for sediment provenance changes

The four units could be distinguished based on the characterization of the major sediment source changes in the CYSM over the last 15.5 kyr (Figs. 4–6). Identification of sediment sources is a useful method for understanding paleo-environmental dynamics and sediment transport mechanisms in the Yellow Sea since the late last deglaciation. The main factors that potentially influenced provenance changes in the Yellow Sea include pronounced sea-level fluctuations that regulate the positions of shorelines, paleo-river pathways, tidal stress amplitude, and the formation of modern ocean currents (Liu *et al*., 2004; Lim *et al*, 2007, 2015; Choi *et al*., 2010; Wang *et al*., 2014; Yoo *et al*., 2015, 2016). Here, we discuss how these complex processes have affected sedimentation in the CYSM during the last 15.5 kyr.

The sea level during Units 3 and 4, which corresponds to the late last deglaciation (15.5–12.1 ka), was approximately 60–100 m lower than the present sea level (Li *et al*., 2014b). The high signatures of C/N values in Unit 4 indicated a significant influx of terrigenous materials (Badejo *et al*., 2016). Mixed deposits of fine and coarse sediments with high influx and sedimentation rates (Figs. 2 and 3) allows us to infer Unit 4 as a delta or prodelta environment. The paleo-river pathways of potential provenances, recently reconstructed based on seismic profiles, merged around the study area and were connected to the East China Sea (Yoo *et al*., 2015, 2016). During sedimentation of Unit 4, sediments in the study area would have been affected most strongly by direct inflow from paleo-rivers, because the low sea level led to the exposure of shelves in and near the Yellow Sea (Li *et al*., 2014b).

Sediment fining during Unit 3 reflects an increase in distance between the river mouths and study area due to transgression, and the study area probably formed a mud flat during sedimentation of Unit 3. During this period, clay-sized particles were still supplied from all rivers (Fig. 4), while silt-sized particles were supplied only from the Huanghe (Fig. 5). The record for the same period in core EZ06-1 showed significant coarse sediments with a high sand content (Lim *et al*., 2015), indicating that the Huanghe was relatively close to the west side of the study area (Fig. 2). In addition, the substantial flux from the Huanghe would have supported the distant movement of coarse grains.

In Unit 2 (12.1–8.8 ka), corresponding to the early Holocene, the sea level was approximately 20−60 m lower than at present (Li *et al*., 2014b). The Unit 2 period was thought to be cold and dry (Badejo *et al*., 2016) and was characterized by oscillating grain sizes and clay mineral and geochemical compositions (Fig. 3). In addition, increasing and decreasing trends of grain size with sand content, S/I ratio divided into two subsections (Fig. 3). This variation is also reported in the surrounding YSC-1 (Li *et al*., 2014a) EZ06-1, and EZ06-2 cores. In this period, the low sea level led to the seaward progradation of the shoreline and formation of a thin sand layer (generally < 3 m) called the transgressive deposit throughout the Yellow Sea (Cummings *et al*., 2016). The change in the coastline configuration caused shifts of the tidal fields therein, with tidal currents being more energetic than at present (Uehara and Saito, 2003; Lim *et al*., 2015), which supplied coarse grains to the central Yellow Sea. In addition, the bottom stress in the Unit 2 period was stronger around the Korean Peninsula (Uehara and Saito, 2003), which caused most of the coarse sediment to be of western Korean river origin (Fig. 6). The supply of fine sediments from the Huanghe was temporarily strengthened during sedimentation of Unit 2-2, but weakened in Unit 2-1 (Fig. 4). This could be due to a change in distance between the Huanghe and study area as the sea level rose. In addition, the paleo-Changjiang Shoal moved northeastward into the Yellow Sea at ~12 ka (Li *et al*., 2000) and may have contributed some materials to the study area (Lim *et al*., 2015). The reduction in Huanghe-derived materials due to the increased distance could be strengthen the influence of the Changjiang in Unit 2-1.

Since sedimentation of Unit 1 (< 8.8 ka), the sea level rose slowly from −20 m to the present level (Li *et al*., 2014b). The tidal field of the Yellow Sea became similar to that of the present (Uehara and Saito, 2003), leading to obviously decreasing contributions from sea bed erosion. A modern-type circulation in the Yellow Sea may have developed between 8.47 and 6.63 ka, characterized by an increase in bottom-water salinity (Kim and Kucera, 2000). The clay minerals and geochemical composition generally point to the Changjiang, with minor influence from the western Korean rivers (Figs. 4 and 6), which is consistent with the reported 'multiple origin' concept (Wei *et al*., 2003; Li *et al*., 2014a; Lim *et al*., 2015; Koo *et al*., 2018). Therefore, the formation of the CYSM and modern ocean circulation could have been synchronic around ~8 ka. The timing of mud patch formation in the central Yellow Sea was inferred to be 9~8 ka with low tidal bottom stress (< 0.35 N/m$^2$) (Uehara and Saito, 2003), which is consistent with our results.

The YSWC played a major role in the unique passage of sediment into the study area since the Unit 1 (Li *et al*., 2014a; Lim *et al*., 2015; Koo *et al*., 2018). The Changjiang Diluted Water can spread some finer sediments to Cheju and nearby areas (Hwang *et al*., 2014; Kwak *et al*., 2014; Li *et al*., 2014a; Lim *et al*., 2015; Koo *et al*., 2018). And then, fine-grained materials could be carried northward along the YSWC path to the CYSM, where the weak tidal-current system and cyclonic eddies provided favorable environment for the formation and maintenance of muddy sedimentations (Shi *et al*., 2003; Lim *et al*., 2015). Meanwhile, barrier effect of oceanic fronts and strong coastal currents restricts to enter the sediments from the Huanghe and western Korean rivers into the CYSM (Li *et al*., 2014a; Koo *et al*., 2018). However, some fine-grained particles from western Korean rivers may influence the CYSM through the Transversal Current (Hwang *et al*., 2014; Koo *et al*., 2018).

**6. Conclusions**

The purpose of this study is to better understand the CYSM in terms of provenance changes and transport mechanisms and to reconstruct the paleo-environment of the Yellow Sea since late last deglaciation using clay mineralogy and geochemical indices from core PCL14. The major conclusions are as follows.

Core PCL14 provides a continuous record of the late last deglaciation to Holocene in the CYSM. The core could be divided mainly into four units: Unit 4 (700–520 cm; 15.5–14.8 ka), Unit 3 (520–280 cm; 14.8–12.1 ka), Unit 2 (280–130 cm; 12.1–8.8 ka), and Unit 1 (130–0 cm; < 8.8 ka). The integration of clay mineralogical and geochemical data distinguished the CYSM sediments into different provenances by grain size. In fine particles, Unit 3 and 4 sediments originated from all possible provenances in the Korea and China, after which the sediment source is gradually shifted to the Changjiang. The inflow of Huanghe-derived fine sediments temporarily increased during Unit 2. On the other hand, the origin of coarse sediments changed in order of all possible rivers (Unit 4), Huanghe (Unit 3), and western Korean rivers (Unit 2). Change in sediment supply are closely related to variations in sea level, positions of paleo-river mouths and tidal stress. Meanwhile, our data suggest that the formation of modern CYSM mud deposition began around ~8 ka with modern ocean circulation and the CYSM sediments are composed mainly of the Changjiang.

**Author contribution**

H.G.Cho designed the experiment, and H.J. Koo carried them out and wrote the paper. All authors contributed to interpreting and discussing the results and reviewing the paper.

**Competing interests**

The authors declare that they have no conflict of interest

**Acknowledgements**

275     This study was supported by the Basic Science Research Program through the National Research Foundation of Korea (NRF) funded by the Ministry of Education, Science and Technology (2017R1D1A1B03027818) and Korea Polar Research Institute project PM16050 funded by the Ministry of Oceans and Fisheries, Korea.

**References**

Badejo, A.O., Choi, B.-H., Cho, H.-G., Yi, H.-I., and Shin, K.-H.: Environmental change in Yellow Sea during the last
280     deglaciation to the early Holocene (15,000-8,000 BP), Quat. Int., 392, 112–124, https://doi.org/10.1016/j.quaint.2015.07.060, 2016.

Beardsley, R.C., Limeburner, R., Yu, H. and Cannon, G.A.: Discharge of the Changjiang (Yangtze River) into the East China Sea, Cont. Shelf Res., 4, 57–76, https://doi.org/10.1016/0278-4343(85)90022-6, 1985.

Biscaye, P.E.: Mineralogy and sedimentation of recent deep-sea clay in the Atlantic Ocean and adjacent seas and oceans, Geol.
285     Soc. Am. Bull., 76, 803–832, https://doi.org/10.1130/0016-7606(1965)76[803:MASORD]2.0.CO;2, 1965.

Blum, J. and Erel, Y.: Radiogenic isotopes in weathering and hydrology, Treatise on geochemistry, 5, 365–392. https://doi.org/10.1016/B0-08-043751-6/05082-9, 2003.

Cho, H.G., Kim, S.-O., Kwak, K.Y. and Choi, H.: Clay mineral distribution and provenance in the Heuksan mud belt, Yellow Sea, Geo-Mar. Lett., 35, 411–419, https://doi.org/10.1007/s00367-015-0417-3, 2015.

290   Choi, J.Y., Lim, D.I., Park, C.H., Kim, S.Y., Kang, S. and Jung, H.S.: Characteristics of clay mineral compositions in river sediments around the Yellow Sea and its application to the provenance of the continental shelf mud deposit, J. Geol. Soc. Korea, 46, 497–509, 2010.

Cummings, D., Dalrymple, R., Choi, K. and Jin, J.: The Tide-Dominated Han River Delta, Korea: Geomorphology, Sedimentology, and Stratigraphic Architecture, Elsevier, Amsterdam, 382 pp, 2016.

295   Duck, R.W., Rowan, J.S., Jenkins, P.A. and Youngs, I.: A multi-method study of bed load provenance and transport pathways in an estuarine channel, Phys. Chem. Earth, 26, 747–752, https://doi.org/10.1016/S1464-1909(01)00080-6, 2001.

Dong, Y.G., Guan, W.G., Chen, Q., Li, X.H., Liu, X.H. and Zeng, X.M.: Sediment transport in the Yellow Sea and East China Sea, Estuar. Coast. Shelf Sci., 93, 248–258, https://doi.org/10.1016/j.ecss.2011.04.003, 2011.

Dou, Y., Yang, S., Liu, Z., Chlift, P.D., Yu, H., Berne, S. and Shi, X.: Clay mineral evolution in the central Okinawa Trough
300     since 28 ka: implications for sediment provenance and paleoenvironmental change, Palaeogeogr. Palaeoclimatol. Palaeoecol., 288, 108–117, https://doi.org/10.1016/j.palaeo.2010.01.040, 2010.

Ha, H.J., Chun, S.S. and Chang, T.S.: Distribution pattern, geochemical composition, and provenance of the Huksan Mud Belt Sediments in the Southeastern Yellow Sea, J. Korean Earth Sci. Soc., 34, 289–302, https://doi.org/10.5467/JKESS.2013.34.4.289, 2013.

305   Hamilton, P., O'nions, R., Bridgwater, D. and Nutman, A.: Sm–Nd studies of Archaean metasediments and metavolcanics from West Greenland and their implications for the Earth's early history, Earth Planet. Sci. Lett., 62, 263–272, https://doi.org/10.1016/0012-821X(83)90089-4, 1983.

Hu, B.Q., Yang, Z.S., Zhao, M.X., Saito, Y., Fan, D.J. and Wang, L.B.: Grain size records reveal variability of the East Asian Winter Monsoon since the Middle Holocene in the Central Yellow Sea mud area, Sci. China Earth Sci., 55, 1656–1668,
310     https://doi.org/10.1007/s11430-012-4447-7, 2012.

Hu, B.Q., Yang, Z.S., Qiao, S.Q., Zhao, M.X., Fan, D.J., Wang, H.J., Bi, N.S. and Li, J.: Holocene shifts in riverine fine-grained sediment supply to the East China Sea Distal Mud in response to climate change, Holocene, 24, 1253–1268, https://doi.org/10.1177/0959683614540963, 2014.

315 Hu, B., Li, J., Zhao, J., Yan, H., Zou, L., Bai, F., Xu, F., Yin, X. and Wei, G.: Sr–Nd isotopic geochemistry of Holocene sediments from the South Yellow Sea: Implications for provenance and monsoon variability, Chem. Geol., 479, 102–112, https://doi.org/10.1177/0959683614540963, 2018.

Huang, D., Zhang, T. and Zhou, F.: Sea-surface temperature fronts in the Yellow and East China Seas from TRMM microwave imager data, Deep-Sea Res. Part II-Top. Stud. Oceanogr., 57, 1017–1024, https://doi.org/10.1016/j.dsr2.2010.02.003, 2010.

320 Hwang, J.H., Van, S.P., Choi, B.-J., Chang, Y.S. and Kim, Y.H.: The physical processes in the Yellow Sea, Ocean Coastal Manage., 102, 449–457, https://doi.org/10.1016/j.ocecoaman.2014.03.026, 2014.

Jung, H.-S., Lim, D., Choi, J.-Y., Yoo, H.-S., Rho, K.-C. and Lee, H.-B.: Rare earth element compositions of core sediments from the shelf of the South Sea, Korea: Their controls and origins, Cont. Shelf Res., 48, 75–86, https://doi.org/10.1016/j.csr.2012.08.008, 2012.

325 KIGAM (Korea Institute of Geology, Mining and Materials): Marine geological study of the continental shelf off Kunsan, West Coast, Korea, KIGAM Technical Report KR-93-5A, Daejeon, Korea, 261 pp, 1993.

Kim, J.-M. and Kucera, M.: Benthic foraminifer record of environmental changes in the Yellow Sea (Hwanghae) during the last 15,000 years, Quat. Sci. Rev., 19, 1067–1085, https://doi.org/10.1016/S0277-3791(99)00086-4, 2000.

Koo, H.J., Lee, Y.J., Kim, S.O. and Cho, H.G.: Clay mineral distribution and provenance in surface sediments of Central 330 Yellow Sea Mud, Geosci. J., 22, 989–1000, https://doi.org/10.1007/s12303-018-0019-y, 2018.

Kwak, K.Y., Choi, H. and Cho, H.G.: Paleo-environmental change during the late Holocene in the southeastern Yellow Sea, Korea, Appl. Clay Sci., 134, 55–61, https://doi.org/10.1016/j.clay.2016.05.007, 2016.

Lee, H.J. and Chough, S.K.: Sediment distribution, dispersal and budget in the Yellow Sea, Mar. Geol., 87, 195–205, https://doi.org/10.1016/0025-3227(89)90061-3, 1989.

335 Li, C.X., Chen, Q.Q., Zhang, J.Q., Yang, S.Y. and Fan, D.D.: Stratigraphy and paleoenvironmental changes in the Yangtze Delta during the Late Quaternary, J. Asian Earth Sci., 18, 453–469, https://doi.org/10.1016/S1367-9120(99)00078-4, 2000.

Li, T.G., Nan, Q.Y., Jiang, B., Sun, R.T., Zhang, D.Y. and Li, Q.: Formation and evolution of the modern warm current system in the East China Sea and the Yellow Sea since the last deglaciation, Chin. J. Oceanol. Limnol., 27, 237–249, 340 https://doi.org/10.1007/s00343-009-9149-4, 2009.

Li, J., Hu, B.Q., Wei, H.L., Zhao, J.T., Zou, L., Bai, F.L., Dou, Y.U., Wang, L.B. and Fang, X.S.: Provenance variations in the Holocene deposits from the southern Yellow Sea: clay mineralogy evidence, Cont. Shelf Res., 90, 41–51, https://doi.org/10.1016/j.csr.2014.05.001, 2014a.

Li, G., Li, P., Liu, Y., Qiqo, L., Ma, Y., Xu, J. and Yang, Z.: Sedimentary system response to the global sea level change in 345 the East China Seas since the last glacial maximum, Earth-Sci. Rev. 139, 390–405, https://doi.org/10.1016/j.earscirev.2014.09.007, 2014b.

Lie, H.-J., Cho, C.-H. and Lee, S.: Frontal circulation and westward transversal current at the Yellow Sea entrance in winter, J. Geophys. Res.-Oceans, 118, 3851–3870, https://doi.org/10.1002/jgrc.20280, 2013.

Lie, H.-J. and Cho, C.-H.: Seasonal circulation patterns of the Yellow and East China Seas derived from satellite-tracked drifter 350 trajectories and hydrographic observations, Prog. Oceanogr., 146, 121–141, https://doi.org/10.1016/j.pocean.2016.06.004, 2016.

Lim, D.J., Choi, J.Y., Jung, H.S., Rho, K.C. and Ahn, K.S.: Recent sediment accumulation and origin of shelf mud deposits in the Yellow and East China Seas, Prog. Oceanogr., 73, 145–159, https://doi.org/10.1016/j.pocean.2007.02.004, 2007.

Lim, D., Jung, H.S. and Choi, J.Y.: REE partitioning in riverine sediments around the Yellow Sea and its importance in shelf
355     sediment provenance, Mar. Geol., 357, 12–24, https://doi.org/10.1016/j.margeo.2014.07.002, 2014.

Lim, D.I., Xu, Z.K., Choi, J.Y., Li, T.G. and Kim, S.Y.: Holocene changes in detrital sediment supply to the eastern part of
the central Yellow Sea and their forcing mechanisms, J. Asian Earth Sci., 150, 18–31,
https://doi.org/10.1016/j.jseaes.2015.03.032, 2015.

Liu, J.P., Milliman, J.D. and Gao, S.: The Shandong mud wedge and post-glacial sediment accumulation in the Yellow Sea,
360     Geo-Mar. Lett., 21, 212–218, https://doi.org/10.1007/s00367-001-0083-5, 2002.

Liu, J.P., Milliman, J.D., Gao, S. and Cheng, P.: Holocene development of the Yellow River's subaqueous delta, North Yellow
Sea, Mar. Geol., 209, 45–67, https://doi.org/10.1016/j.margeo.2004.06.009, 2004.

Liu, J., Saito, Y., Wang, H., Yang, Z. and Nakashima, R.: Sedimentary evolution of the Holocene subaqueous clinoform off
the Shandong Peninsula in the Yellow Sea, Mar. Geol., 236, 165–187, https://doi.org/10.1016/j.margeo.2006.10.031,
365     2007.

Liu, J., Saito, Y., Kong, X., Wang, H., Wen, C., Yang, Z. and Nakashima, R.: Delta development and channel incision during
marine isotope stage 3 and 2 in the western South Yellow Sea, Mar. Geol., 278, 54–76,
https://doi.org/10.1016/j.margeo.2010.09.003, 2010a.

Liu, Z., Colin, C., Li, X., Zhao, Y., Tuo, S., Chen, Z., Siringan, F. P., Liu, J. T., Huang, C.-Y., You, C.-F., You, C.-F. and
370     Huang, K.-F.: Clay mineral distribution in surface sediments of the northeastern South China Sea and surrounding fluvial
drainage basins: Source and transport, Mar. Geol., 277, 48–60, https://doi.org/10.1016/j.margeo.2010.08.010, 2010b.

Liu, S., Shi, X., Fang, X., Dou, Y., Liu, Y. and Wang, X.: Spatial and temporal distributions of clay minerals in mud deposits
on the inner shelf of the East China Sea: Implications for paleoenvironmental changes in the Holocene. Quat. Int., 349,
270–279, https://doi.org/10.1016/j.quaint.2014.07.016, 2014.

375   McLennan, S.M.: Rare earth elements in sedimentary rocks: influence of provenance and sedimentary processes, in:
Geochemistry and mineralogy of rare earth elements, edited by: Lipin, B.R. and McKay, G.A., Reviews in Mineralogy,
21, Mineralogy Society of America, Washington, DC, 169–200, 1989.

Milliman, J.D., Shen, H.T., Yang, Z.S. and Mead, R.H.: Transport and deposition of river sediment in the Changjiang estuary
and adjacent continental shelf, Cont. Shelf Res., 4, 37–45, https://doi.org/10.1016/0278-4343(85)90020-2, 1985.

380   Milliman, J.D., Qin, Y.S., Ren, M.E. and Saito, Y.: Man's influence on the erosion and transport of sediment by Asian rivers:
the Yellow River (Huanghe) example, J. Geol., 95, 751–762, https://doi.org/10.1086/629175, 1987.

Shi, X.F., Shen, S.X., Yi, H.-I., Chen, Z.H. and Meng, Y.: Modern sedimentary environments and dynamic depositional
systems in the southern Yellow Sea, Chin. Sci. Bull., 48, 1–7, https://doi.org/10.1007/BF02900933, 2003.

Shinn, Y.J., Chough, S.K., Kim, J.W. and Woo, J.: Development of depositional systems in the southeastern Yellow Sea during
385     the postglacial transgression, Mar. Geol., 239, 59–82, https://doi.org/10.1016/j.margeo.2006.12.007, 2007.

Song, Y.-H. and Choi, M.S.: REE geochemistry of fine-grained sediments from major rivers around the Yellow Sea. Chem.
Geol., 266, 328–342, https://doi.org/10.1016/j.chemgeo.2009.06.019, 2009.

Uehara, K. and Saito, Y.: Late Quaternary evolution of the Yellow/East China Sea tidal regime and its impacts on sediment
dispersal and seafloor morphology, Sediment. Geol., 162, 25–38, https://doi.org/10.1016/S0037-0738(03)00234-3, 2003.

390   Wang, L., Sarnthein, M., Erlenkeuser, H., Grimalt, J., Grootes, P., Heilig, S., Ivanova, E., Kienast, M., Pelejero, C. and
Pflaumann, U.: East Asian monsoon climate during the Late Pleistocene: high-resolution sediment records from the South
China Sea, Mar. Geol., 156, 245–284, https://doi.org/10.1016/S0025-3227(98)00182-0, 1999.

Wang. L., Yang, Z., Zhang, R.P., Fan, D.J., Zhao, M.X. and Hu, B.Q.: Sea surface temperature records of core ZY2 from the
central mud area in the South Yellow Sea during last 6200 years and related effect of the Yellow Sea Warm Current,
395     Chin. Sci. Bull., 56, 1588–1595, https://doi.org/10.1007/s11434-011-4442-y, 2011.

Wang, F., Liu, C. and Meng, Q.: Effect of the Yellow Sea warm current fronts on the westward shift of the Yellow Sea warm tongue in winter, Cont. Shelf Res., 45, 98–107, https://doi.org/10.1016/j.csr.2012.06.005, 2012.

Wang, Q. and Yang, S.Y.: Clay mineralogy indicates the Holocene monsoon climate in the Changjiang (Yangtze River) Catchment, China, Appl. Clay Sci., 74, 28–36, https://doi.org/10.1016/j.clay.2012.08.011, 2013.

400  Wang, Y., Li, G., Zhang, W. and Dong, P.: Sedimentary environment and formation mechanism of the mud deposit in the central South Yellow Sea during the past 40 kyr, Mar. Geol., 347, 123–135, https://doi.org/10.1016/j.margeo.2013.11.008, 2014.

Wei, J.W., Shi, X.F., Li, G.X. and Liang, R.C.: Clay mineral distributions in the southern Yellow Sea and their significance, Chin. Sci. Bull., 48, 7–11, https://doi.org/10.1007/BF02900934, 2003.

405  Xiang, R., Yang, Z.S., Saito, Y., Fan, D.J., Chen, M.H., Guo, Z.G. and Chen, Z.: Paleoenvironmental changes during the last 8400 years in the southern Yellow Sea: Benthic foraminiferal and stable isotopic evidence, Mar. Micropaleontol., 67, 104–119, https://doi.org/10.1016/j.marmicro.2007.11.002, 2008.

Xu, D., Liu, X., Zhang, X., Li, T. and Chen, B.: China Offshore Geology,. Geological Publishing House, Beijing, 310 pp, 1997.

410  Xu, Z.K., Lim, D.I., Choi, J.Y., Yang, S.Y. and Jung, H.J.: Rare earth elements in bottom sediments of major rivers around the Yellow Sea: implications for sediment provenance, Geo-Mar. Lett., 29, 291–300, https://doi.org/10.1007/s00367-009-0142-x, 2009.

Xu, Z.K., Li, T.G., Chang, F.M., Wan, S.M., Choi, J.Y. and Lim, D.I.: Clay-sized sediment provenance change in the northern Okinawa Trough since 22 kyr BP and its paleoenvironmental implication, Palaeogeogr. Palaeoclimatol. Palaeoecol., 399, 415  236–245, https://doi.org/10.1016/j.palaeo.2014.01.016, 2014.

Yang, Y.S., Jung, H.S., Choi, M.S. and Li, C.X.: The rare earth element compositions of the Changjiang (Yangtze) and Huanghe (Yellow) river sediments, Earth Planet. Sci. Lett., 201, 407–419, https://doi.org/10.1016/S0012-821X(02)00715-X, 2002.

Yang, S.Y., Jung, H.S., Lim, D.I. and Li, C.X.: A review on the provenance discrimination of sediments in the Yellow Sea. 420  Earth-Sci. Rev., 63, 93–120, https://doi.org/10.1016/S0012-8252(03)00033-3, 2003.

Yang, Z.S. and Liu, J.P.: A unique Yellow River-derived distal subaqueous delta in the Yellow Sea. Mar. Geol., 240, 169–176, https://doi.org/10.1016/j.margeo.2007.02.008, 2007.

Yang, S.Y. and Youn, J.-S.: Geochemical compositions and provenance discrimination of the central south Yellow Sea sediments. Mar. Geol., 243, 229–241, https://doi.org/10.1016/j.margeo.2007.05.001, 2007.

425  Yoo, D.G., Koo, N.-H., Lee, H.-Y., Kim, B.-Y., Kim, Y.-J. and Cheong, S.: Acquisition, processing and interpretation of high-resolution seismic data using a small-scale multi-channel system: an example from the Korea Strait inner shelf, south-east Korea, Explor. Geophys., 47, 341–351, https://doi.org/10.1071/EG15081, 2015.

Yoo, D.-G., Lee, G.-S., Kim, G.-Y., Kang, N.-K., Yi, B.-Y., Kim, Y.-J., Chun, J.-H. and Kong, G.-S.: Seismic stratigraphy and depositional history of late Quaternary deposits in a tide-dominated setting: An example from the eastern Yellow 430  Sea, Mar. Pet. Geol., 73, 212–227, https://doi.org/10.1016/j.marpetgeo.2016.03.005, 2016.

Zhao, Y.Y., Qin, Z.Y., Li, F.Y. and Chen, Y.W.: On the source and genesis of the mud in the central area of the south Yellow Sea, Chin. J. Oceanol. Limnol., 8, 66–73, https://doi.org/10.1007/BF02846453, 1990.

Zhang, W., Xing, Y., Yu, L., Feng, H. and Lu, M.: Distinguishing sediments from the Yangtze and Yellow Rivers, China: a mineral magnetic approach, Holocene, 18, 1139–1145, https://doi.org/10.1177/0959683608095582, 2008.

435

**Figure captions**

**Figure 1.** Schematic map showing the location of core PCL14 as well as the surface circulation in the Yellow Sea (modified from Li et al., 2014a; Wang et al., 2014). The gray dotted line indicate the paleo-river pathways (Yoo et al., 2016). ① Central Yellow Sea Mud (CYSM); ② Southeastern Yellow Sea Mud (SEYSM); ③ Southwestern Cheju Island Mud (SWCIM); KC = Kuroshio Current; YSWC = Yellow Sea Warm Current; SDCC = Shandong Coastal Current; YSCC = Yellow Sea Coastal Current; KCC = Korean Coastal Current; SDF = Shandong Front; JSCF = Jiangsu Coastal Front; WKCF = Western Korean Coastal Front.

**Figure 2.** (a) Isolines in thickness of mud deposit CYSM (after Wang et al., 2014), (b) vertical lithology profile of core PCL14, YSC-1 (Li et al., 2014a) and EZ06 cores (Lim et al., 2015).

**Figure 3.** Downcore variations of mean grain size, clay mineralogical and geochemical data in core PCL14 with sea level changes (Li et al., 2014b). Note the overall distribution into four units.

**Figure 4.** Ternary diagrams showing variations in clay mineral compositions of core PCL14. Published data of potential source sediments including the Changjiang, Huanghe, and western Korean rivers (the Han, Keum, and Yeongsan Rivers) (Cho et al., 2015; Koo et al., 2018), which are plotted for comparison.

**Figure 5.** Correlation plots of grain size or clay/silt ratio with (a) major elements, (b) Zr/Th and La/Sc, (c) UCC-normalized REEs, and (d) $^{87}Sr/^{86}Sr$ and εNd for core PCL14.

**Figure 6.** Discrimination plots showing variations in (a) $\sum LREE/Yb$ *vs.* $(La/Lu)_{UCC}$, (b) $(La/Yb)_{UCC}$ *vs.* εNd, and (c) (smectite+kaolinite+chlorite)/illte *vs.* εNd. Clay mineral (Cho et al., 2015; Koo et al., 2018), rare earth element (Xu et al., 2009), and isotope data of potential sources are also shown for comparison.

**Fig. 7.** Schematic diagram showing the influence of shoreline changes, and paleo-river pathways on riverine sediment supplied to the study area during (a) Unit 4 and 3 (15.5–12.1 ka), (b) Unit 2 (12.1–8.8 ka), and (c) Unit 1 (8.8 ka–present) (modified Lim et al., 2015).
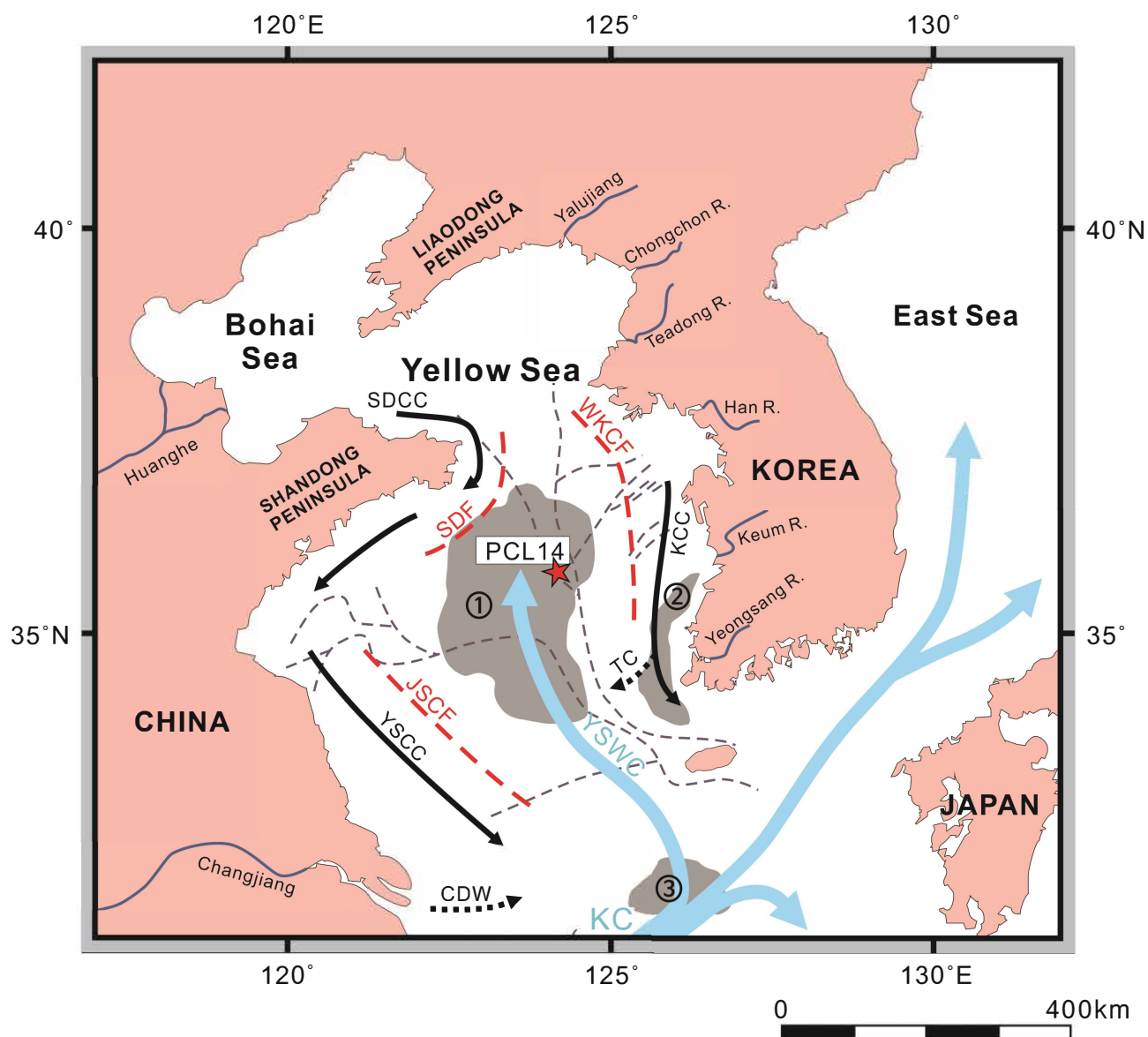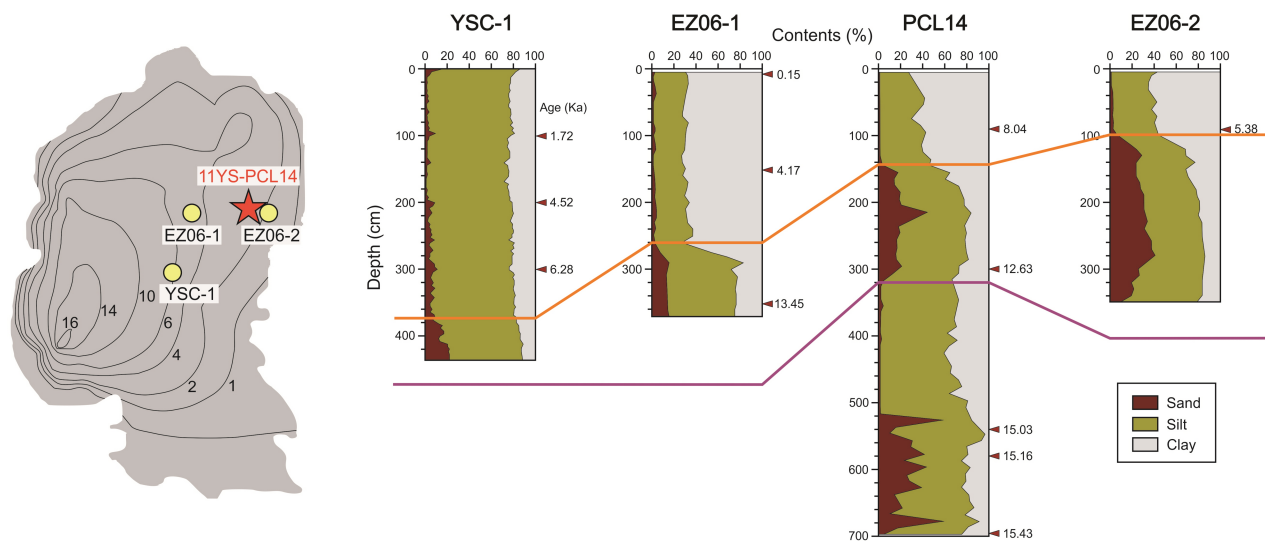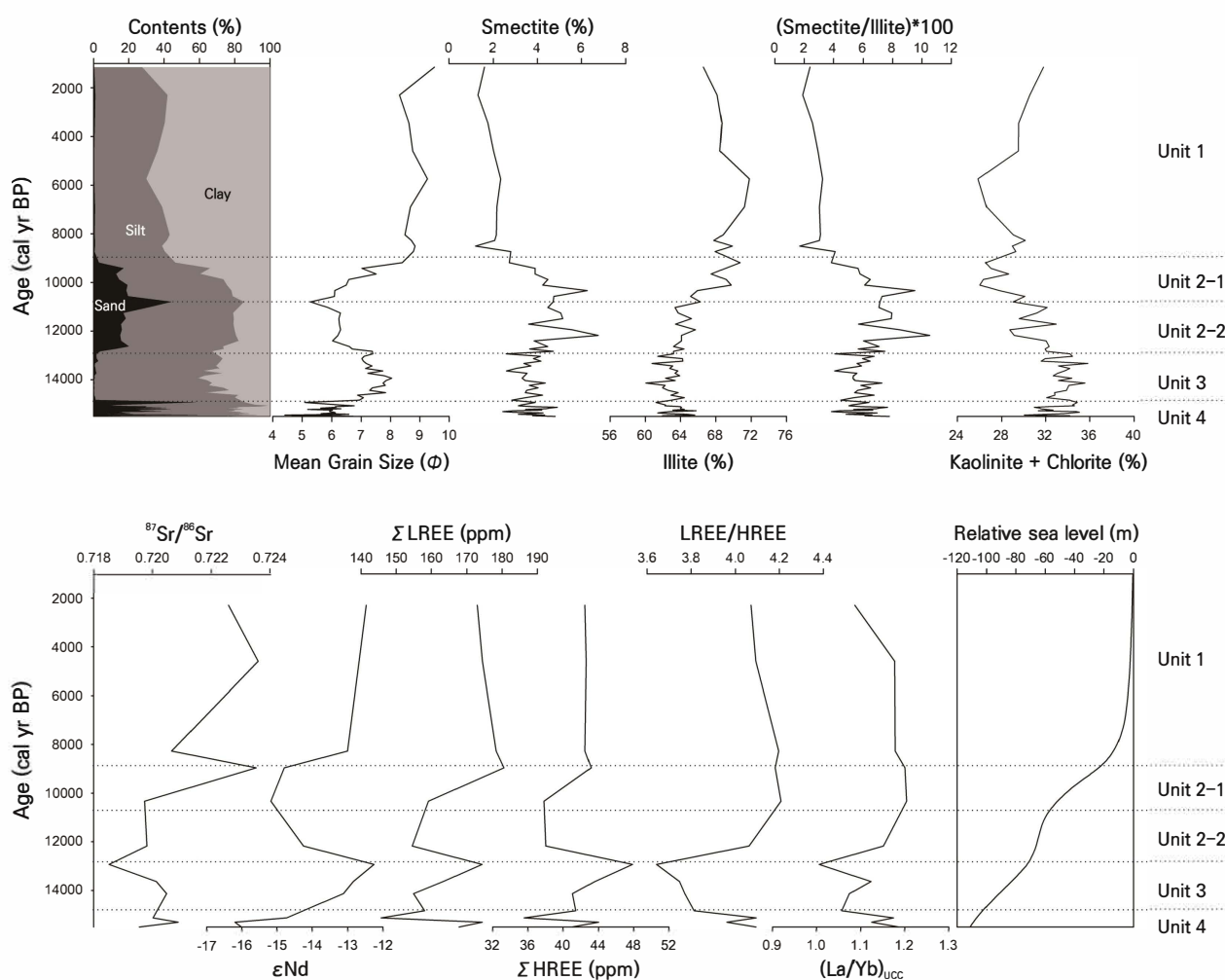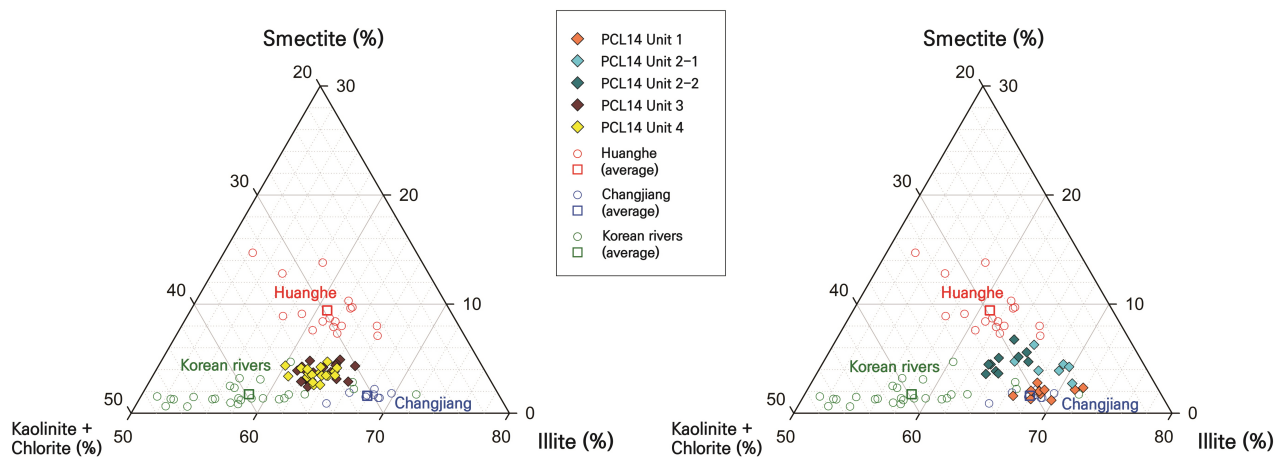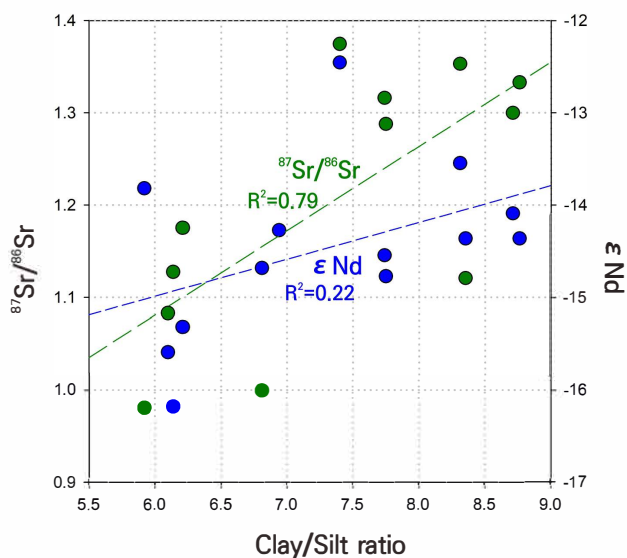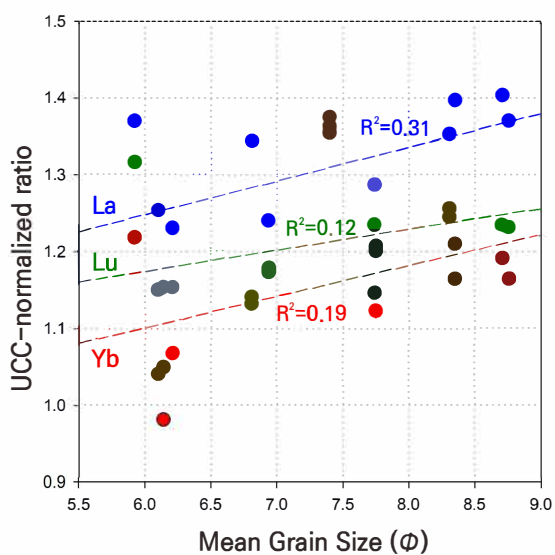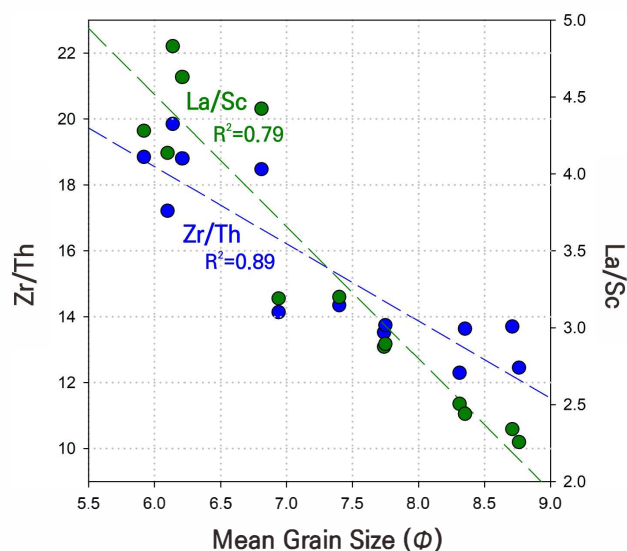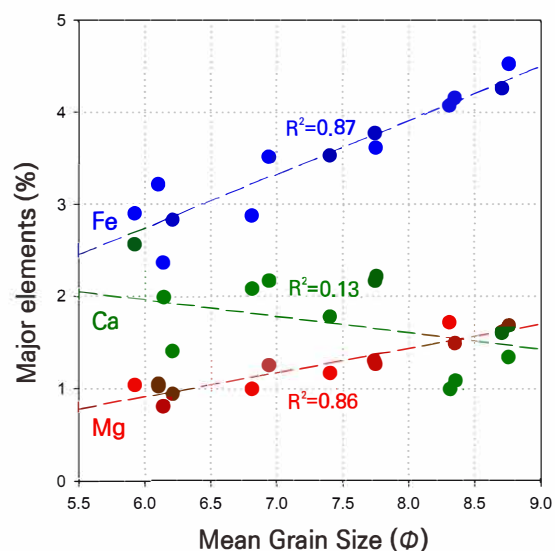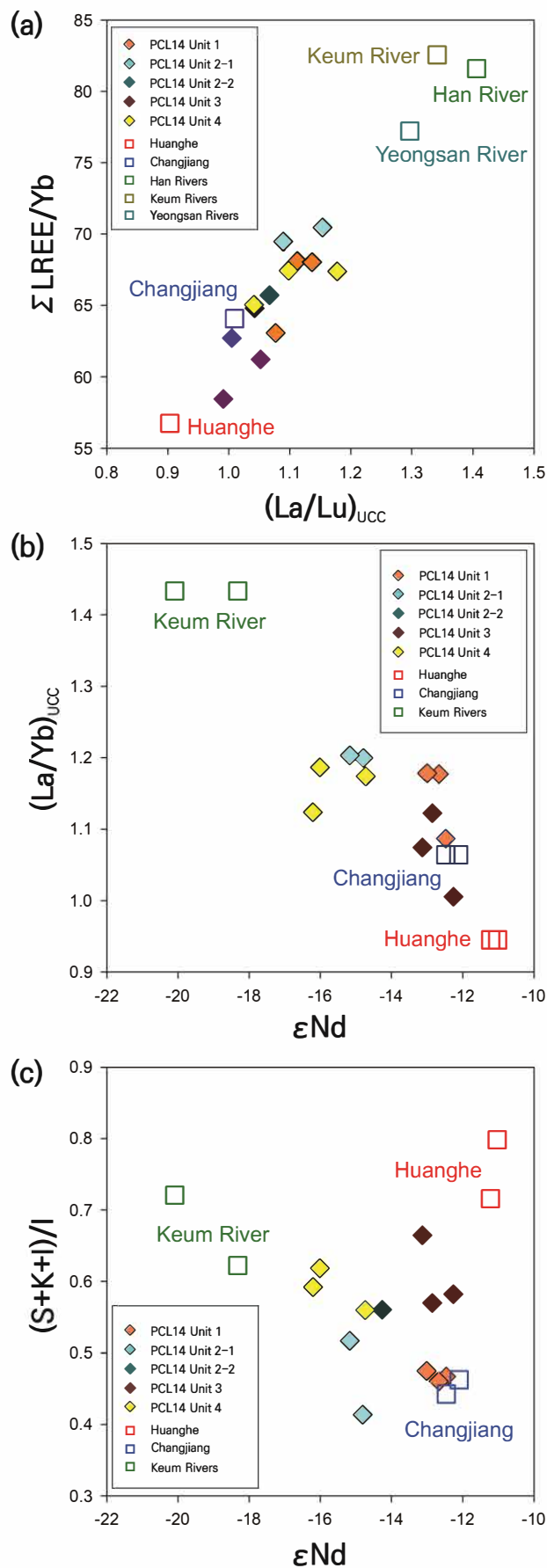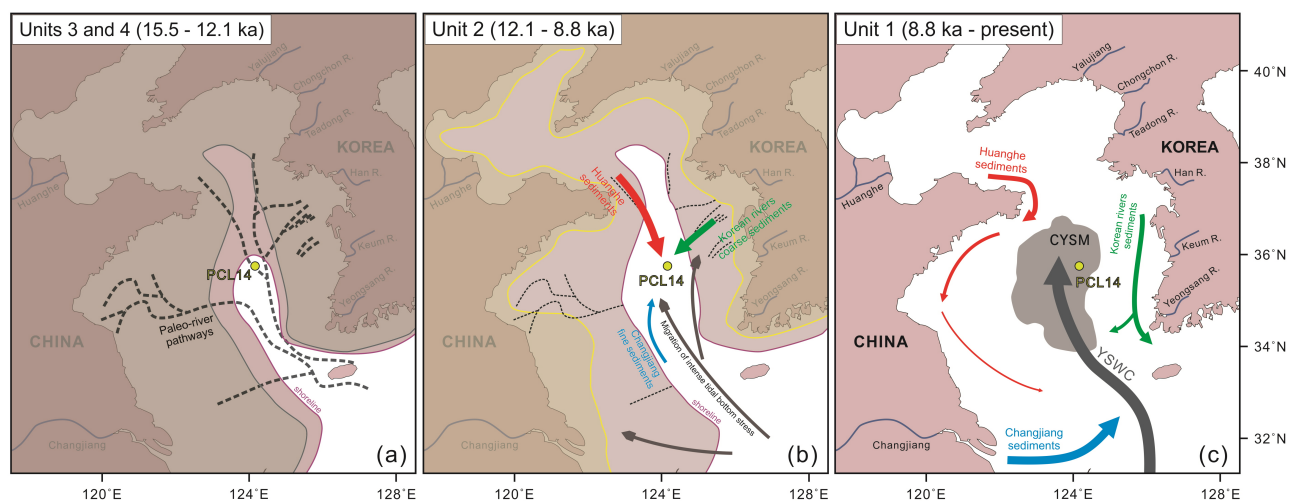
Table 1. Representative accelerator mass spectrometer radiocarbon age data for core PCL14 from Badejo et al. (2016). OM = organic matter, Cali. Age = calibrated age.

| Core | Depth (cm) | Sample type | $^{14}$C age (yr BP) | Cali. age (cal.yr.BP) ± 95% probability |
|------|-----------|-------------|---------------------|------------------------------------------|
| | 90 | OM | 7,160 ± 40 | 8,040 ± 90 |
| | 300 | Shell | 10,360 ±40 | 12,630 ± 190 |
| 11 YS PCL 14 | 540 | Shell | 12,400 ±50 | 15,030 ± 290 |
| | 580 | Shell | 12,530 ±50 | 15,160 ± 210 |
| | 698 | Shell | 12,720 ±50 | 15,430 ± 250 |

Table 2. Average compositions of clay minerals in core PCL14 sediments and their potential provenance rivers.

| Samples | $n$ | Illite (%) | Chlorite (%) | Kaolinite (%) | Smectite (%) | Reference |
|---------|-----|-----------|-------------|---------------|--------------|-----------|
| PCL14_Unit 1 | 9 | 69.0 ± 1.6 | 18.2 ± 1.3 | 10.9 ± 0.6 | 1.8 ± 0.4 | This study |
| PCL14_Unit 2 | 16 | 67.0 ± 3.0 | 16.5 ± 2.3 | 12.1 ± 1.2 | 4.5 ± 1.1 | |
| PCL14_Unit 3 | 24 | 63.0 ± 1.1 | 19.7 ± 1.0 | 13.7 ± 0.6 | 3.6 ± 0.5 | |
| PCL14_Unit 4 | 18 | 63.2 ± 1.4 | 20.0 ± 1.3 | 13.0 ± 0.7 | 3.8 ± 0.7 | |
| Changjiang | 9 | 68.1 | 17.0 | 13.3 | 1.6 | Koo et al. (2018) |
| | 8 | 66 | 12 | 16 | 6 | Yang et al. (2003) |
| | - | 61.7 | 24.5 | 9.8 | 3.9 | Choi et al. (2010) |
| Huanghe | 13 | 62.2 | 15.8 | 13.1 | 8.9 | Koo et al. (2018) |
| | 4 | 56.7 | 17.7 | 14.1 | 11.5 | Cho et al. (2015) |
| | 8 | 62 | 16 | 10 | 12 | Yang et al. (2003) |
| Western Korean rivers (Han / Keum / Yeongsan) | 14/9/3 | 59.5 | 21.3 | 17.4 | 1.8 | Cho et al. (2015) |
| | 45 | 52 | 44 | | 4 | Lim et al. (2015) |

Table 3. Isotopic and geochemical data of core PCL14 and riverine samples.

| Samples | $^{87}Sr/^{86}Sr$ ( $\pm 2\sigma \times 10^{6}$) | $^{143}Nd/^{144}Nd$ ( $\pm 2\sigma \times 10^{6}$) | $\varepsilon Nd$ | (La/Yb)ucc | (La/Lu)ucc | $\Sigma LREE/\Sigma HREE$ | $\Sigma LREE/Yb$ |
|---|---|---|---|---|---|---|---|
| PCL14-2 (47 cm) | 0.722591 (14) | 0.511999 (4) | -12.5 | 1.09 | 1.08 | 4.07 | 63.1 |
| PCL14-4 (67 cm) | 0.723603 (11) | 0.511988 (5) | -12.7 | 1.18 | 1.11 | 4.09 | 68.1 |
| PCL14-8 (107 cm) | 0.720661 (11) | 0.511971 (4) | -13.0 | 1.18 | 1.14 | 4.2 | 68.1 |
| PCL14-11 (137 cm) | 0.723536 (17) | 0.511880 (3) | -14.8 | 1.2 | 1.15 | 4.18 | 70.5 |
| PCL14-17 (197 cm) | 0.719741 (11) | 0.511860 (3) | -15.2 | 1.2 | 1.09 | 4.21 | 69.5 |
| PCL14-25 (277 cm) | 0.719819 (14) | 0.511908 (3) | -14.2 | 1.15 | 1.07 | 4.06 | 65.8 |
| PCL14-30 (327 cm) | 0.718528 (27) | 0.512010 (3) | -12.3 | 1.01 | 0.99 | 3.64 | 58.5 |
| PCL14-37 (397 cm) | 0.720141 (7) | 0.511980 (4) | -12.8 | 1.12 | 1.04 | 3.75 | 64.8 |
| PCL14-42 (447 cm) | 0.720495 (50) | 0.511965 (7) | -13.1 | 1.07 | 1.01 | 3.77 | 62.7 |
| PCL14-54 (567 cm) | 0.720030 (8) | 0.511883 (6) | -14.7 | 1.17 | 1.10 | 4.09 | 67.5 |
| PCL14-60 (627 cm) | 0.720886 (8) | 0.511808 (10) | -16.2 | 1.12 | 1.04 | 3.96 | 65.1 |
| PCL14-67 (697 cm) | 0.719559 (8) | 0.511817 (5) | -16.0 | 1.19 | 1.18 | 4.09 | 67.4 |
| Huanghe | 0.717596 (9) | 0.512073 (5) | -11.0 | | | | |
| | 0.717260 (10) | 0.512063 (4) | -11.2 | | | | |
| Changjiang | 0.722954 (8) | 0.511999 (6) | -12.5 | | | | |
| | 0.726349 (7) | 0.512018 (5) | -12.1 | | | | |
| Keum River | 0.724526 (6) | 0.511609 (4) | -20.1 | | | | |
| | 0.724881 (5) | 0.511700 (3) | -18.3 | | | | |